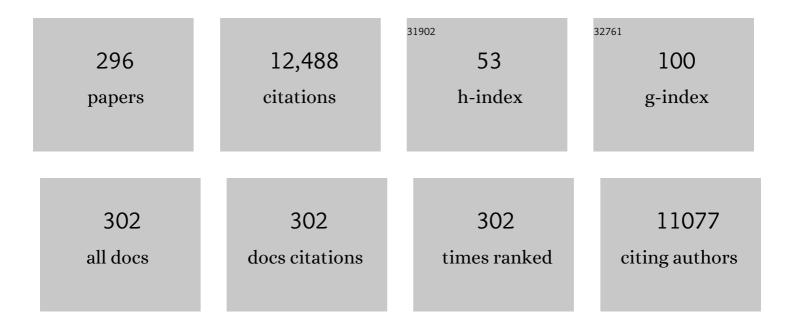
List of Publications by Year in descending order

Source: https://exaly.com/author-pdf/619137/publications.pdf Version: 2024-02-01



#	Article	IF	CITATIONS
1	A benchmark study on the thermal conductivity of nanofluids. Journal of Applied Physics, 2009, 106, .	1.1	897
2	Medical applications of infrared thermography: A review. Infrared Physics and Technology, 2012, 55, 221-235.	1.3	847
3	Infrared thermography for condition monitoring – A review. Infrared Physics and Technology, 2013, 60, 35-55.	1.3	648
4	Review on thermal properties of nanofluids: Recent developments. Advances in Colloid and Interface Science, 2015, 225, 146-176.	7.0	352
5	Enhancement of thermal conductivity in magnetite based nanofluid due to chainlike structures. Applied Physics Letters, 2007, 91, .	1.5	320
6	Effect of clustering on the thermal conductivity of nanofluids. Materials Chemistry and Physics, 2008, 109, 50-55.	2.0	269
7	Thermal properties of nanofluids. Advances in Colloid and Interface Science, 2012, 183-184, 30-45.	7.0	225
8	Evidence for enhanced thermal conduction through percolating structures in nanofluids. Nanotechnology, 2008, 19, 305706.	1.3	224
9	Nanofluid with tunable thermal properties. Applied Physics Letters, 2008, 92, .	1.5	207
10	Effect of initial pH and temperature of iron salt solutions on formation of magnetite nanoparticles. Materials Chemistry and Physics, 2007, 103, 168-175.	2.0	203
11	Inversion of Silica-Stabilized Emulsions Induced by Particle Concentration. Langmuir, 2005, 21, 3296-3302.	1.6	202
12	Synthesis of Aqueous and Nonaqueous Iron Oxide Nanofluids and Study of Temperature Dependence on Thermal Conductivity and Viscosity. Journal of Physical Chemistry C, 2010, 114, 18825-18833.	1.5	173
13	Influence of Co <sup>2+</sup> Ion Concentration on the Size, Magnetic Properties, and Purity of CoFe <sub>2</sub> O <sub>4</sub> Spinel Ferrite Nanoparticles. Journal of Physical Chemistry C, 2010, 114, 6334-6341.	1.5	172
14	Synthesis, characterization, and thermal property measurement of nano-Al95Zn05 dispersed nanofluid prepared by a two-step process. International Journal of Heat and Mass Transfer, 2011, 54, 3783-3788.	2.5	166
15	Role of microconvection induced by Brownian motion of nanoparticles in the enhanced thermal conductivity of stable nanofluids. Applied Physics Letters, 2009, 94, .	1.5	156
16	Effect of Digestion Time and Alkali Addition Rate on Physical Properties of Magnetite Nanoparticles. Journal of Physical Chemistry B, 2007, 111, 7978-7986.	1.2	152
17	Micelle based synthesis of cobalt ferrite nanoparticles and its characterization using Fourier Transform Infrared Transmission Spectrometry and Thermogravimetry. Materials Chemistry and Physics, 2010, 124, 264-269.	2.0	146
18	Correlation between Plantar Foot Temperature and Diabetic Neuropathy: A Case Study by Using an Infrared Thermal Imaging Technique. Journal of Diabetes Science and Technology, 2010, 4, 1386-1392.	1.3	143

#	Article	IF	CITATIONS
19	Infrared thermal imaging for detection of peripheral vascular disorders. Journal of Medical Physics, 2009, 34, 43.	0.1	136
20	Tuning of Thermal Conductivity and Rheology of Nanofluids Using an External Stimulus. Journal of Physical Chemistry C, 2011, 115, 20097-20104.	1.5	132
21	Optical Properties and Applications of Ferrofluids—A Review. Journal of Nanofluids, 2012, 1, 3-20.	1.4	123
22	Magnetically controllable nanofluid with tunable thermal conductivity and viscosity. Applied Physics Letters, 2009, 95, .	1.5	120
23	A tunable optical filter. Measurement Science and Technology, 2003, 14, 1289-1294.	1.4	111
24	Efficient removal of methylene blue dye using cellulose capped Fe3O4 nanofluids prepared using oxidation-precipitation method. Colloids and Surfaces A: Physicochemical and Engineering Aspects, 2019, 567, 193-204.	2.3	109
25	Magnetic nanoparticles with enhanced γ-Fe2O3to α-Fe2O3phase transition temperature. Nanotechnology, 2006, 17, 5851-5857.	1.3	105
26	Effects of Interaction of Ionic and Nonionic Surfactants on Self-Assembly of PEO–PPO–PEO Triblock Copolymer in Aqueous Solution. Journal of Physical Chemistry B, 2012, 116, 1499-1507.	1.2	98
27	Magnetic hyperthermia in phosphate coated iron oxide nanofluids. Journal of Magnetism and Magnetic Materials, 2016, 407, 101-113.	1.0	96
28	Carbon black nano particle loaded lauric acid-based form-stable phase change material with enhanced thermal conductivity and photo-thermal conversion for thermal energy storage. Energy, 2020, 191, 116572.	4.5	91
29	Influence of aggregation on thermal conductivity in stable and unstable nanofluids. Applied Physics Letters, 2010, 97, .	1.5	90
30	Effect of thermal annealing under vacuum on the crystal structure, size, and magnetic properties of ZnFe2O4 nanoparticles. Journal of Applied Physics, 2007, 102, .	1.1	89
31	Nanofluid based optical sensor for rapid visual inspection of defects in ferromagnetic materials. Applied Physics Letters, 2012, 100, .	1.5	89
32	Effect of Surfactant Monolayer on Reduction of Fe <sub>3</sub> O <sub>4</sub> Nanoparticles under Vacuum. Journal of Physical Chemistry C, 2008, 112, 18376-18383.	1.5	88
33	A simple, rapid and single step method for fabricating superhydrophobic titanium surfaces with improved water bouncing and self cleaning properties. Applied Surface Science, 2020, 512, 145636.	3.1	88
34	Experimental evidence for reversible zippering of chains in magnetic nanofluids under external magnetic fields. Physical Review E, 2009, 80, 041401.	0.8	84
35	Room temperature ferromagnetism in vacuum annealed ZnFe2O4 nanoparticles. Applied Physics Letters, 2010, 96, .	1.5	83
36	Template-Free One-Step Electrodeposition Method for Fabrication of Robust Superhydrophobic Coating on Ferritic Steel with Self-Cleaning Ability and Superior Corrosion Resistance. Langmuir, 2019, 35, 12665-12679.	1.6	79

#	Article	IF	CITATIONS
37	Effect of Digestion Time on Size and Magnetic Properties of Spinel CoFe <sub>2</sub> O <sub>4</sub> Nanoparticles. Journal of Physical Chemistry C, 2009, 113, 590-596.	1.5	74
38	A facile method to control the size and magnetic properties of CoFe2O4 nanoparticles. Materials Chemistry and Physics, 2009, 115, 712-717.	2.0	72
39	Recent Advances in Magnetorheology of Ferrofluids (Magnetic Nanofluids)—A Critical Review. Journal of Nanofluids, 2016, 5, 1-22.	1.4	70
40	Three Distinct Scenarios under Polymer, Surfactant, and Colloidal Interaction. Macromolecules, 2003, 36, 9230-9236.	2.2	66
41	Thermal conductivity enhancement in organic phase change material (phenol-water system) upon addition of Al2O3, SiO2 and TiO2 nano-inclusions. Journal of Molecular Liquids, 2018, 269, 47-63.	2.3	66
42	Quantification of defects in composites and rubber materials using active thermography. Infrared Physics and Technology, 2012, 55, 191-199.	1.3	64
43	Robust nickel-reduced graphene oxide-myristic acid superhydrophobic coating on carbon steel using electrochemical codeposition and its corrosion resistance. Surface and Coatings Technology, 2020, 397, 125942.	2.2	64
44	Magnetic hyperthermia in magnetic nanoemulsions: Effects of polydispersity, particle concentration and medium viscosity. Journal of Magnetism and Magnetic Materials, 2017, 441, 310-327.	1.0	62
45	Graphene oxide-chitosan-silver composite coating on Cu-Ni alloy with enhanced anticorrosive and antibacterial properties suitable for marine applications. Progress in Organic Coatings, 2020, 139, 105444.	1.9	62
46	Superior thermal conductivity and photo-thermal conversion efficiency of carbon black loaded organic phase change material. Journal of Molecular Liquids, 2019, 285, 640-657.	2.3	61
47	Polymer-Induced Repulsive Forces: Exponential Scaling. Physical Review Letters, 1998, 80, 1778-1781.	2.9	59
48	Interaction between Emulsion Droplets in the Presence of Polymerâ^'Surfactant Complexes. Langmuir, 2002, 18, 4625-4631.	1.6	59
49	Role of Thermal Conductivity of Dispersed Nanoparticles on Heat Transfer Properties of Nanofluid. Industrial & Engineering Chemistry Research, 2014, 53, 980-988.	1.8	58
50	Magnetic field induced extinction of light in a suspension of Fe3O4 nanoparticles. Applied Physics Letters, 2008, 92, .	1.5	55
51	Probing of Field-Induced Structures and Tunable Rheological Properties of Surfactant Capped Magnetically Polarizable Nanofluids. Langmuir, 2013, 29, 110-120.	1.6	55
52	High performance green concrete (HPGC) with improved strength and chloride ion penetration resistance by synergistic action of fly ash, nanoparticles and corrosion inhibitor. Construction and Building Materials, 2019, 198, 299-312.	3.2	55
53	Light scattering in a magnetically polarizable nanoparticle suspension. Physical Review E, 2008, 78, 031404.	0.8	54
54	Effect of Nanoparticles Aggregation on Thermal and Electrical Conductivities of Nanofluids. Journal of Nanofluids, 2014, 3, 17-25.	1.4	54

#	Article	IF	CITATIONS
55	X-ray diffraction-based characterization of magnetite nanoparticles in presence of goethite and correlation with magnetic properties. Physica E: Low-Dimensional Systems and Nanostructures, 2007, 39, 20-25.	1.3	53
56	Effect of Hydrophilic Silica Nanoparticles on the Magnetorheological Properties of Ferrofluids: A Study Using Opto-magnetorheometer. Langmuir, 2015, 31, 3343-3353.	1.6	51
57	Effect of divalent metal hydroxide solubility product on the size of ferrite nanoparticles. Materials Letters, 2007, 61, 4545-4548.	1.3	49
58	Sensing of Biologically Important Cations Such as Na <sup>+</sup> , K <sup>+</sup> , Ca <sup>2+</sup> , Cu <sup>2+</sup> , and Fe <sup>3+</sup> Using Magnetic Nanoemulsions. Langmuir, 2013, 29, 4252-4258.	1.6	49
59	Synthesis, characterization and antimicrobial property of Fe3O4-Cys-HNQ nanocomplex, with I-cysteine molecule as a linker. RSC Advances, 2013, 3, 8047.	1.7	49
60	The effect of suspended Fe3O4 nanoparticle size on magneto-optical properties of ferrofluids. Optics Communications, 2015, 336, 278-285.	1.0	49
61	Stretching and Collapse of Neutral Polymer Layers under Association with Ionic Surfactants. Physical Review Letters, 2002, 89, 268301.	2.9	48
62	Self-assembly of surfactin in aqueous solution: Role of divalent counterions. Colloids and Surfaces B: Biointerfaces, 2014, 116, 396-402.	2.5	47
63	Kerr-effect investigations in a nematic liquid crystal. Physical Review A, 1992, 46, 2163-2165.	1.0	44
64	Enhanced seawater corrosion resistance of reinforcement in nanophase modified fly ash concrete. Construction and Building Materials, 2019, 221, 232-243.	3.2	44
65	Fabrication of superhydrophobic titanium surfaces with superior antibacterial properties using graphene oxide and silanized silica nanoparticles. Surface and Coatings Technology, 2020, 400, 126074.	2.2	44
66	A new optical technique for detection of defects in ferromagnetic materials and components. NDT and E International, 2000, 33, 289-295.	1.7	43
67	Measurement of thermal diffusivity of solids using infrared thermography. Materials Letters, 2008, 62, 2740-2742.	1.3	42
68	Experimental investigation of magnetic-field-induced aggregation kinetics in nonaqueous ferrofluids. Physical Review E, 2010, 82, 021402.	0.8	41
69	Effect of phosphate and oleic acid capping on structure, magnetic properties and thermal stability of iron oxide nanoparticles. Journal of Alloys and Compounds, 2016, 689, 959-968.	2.8	41
70	Assessment of long term stability of aqueous nanofluids using different experimental techniques. Journal of Molecular Liquids, 2016, 222, 350-358.	2.3	41
71	Magnetic hyperthermia study in water based magnetic fluids containing TMAOH coated Fe3O4 using infrared thermography. Infrared Physics and Technology, 2017, 80, 71-82.	1.3	41
72	A methanol sensor based on stimulus-responsive magnetic nanoemulsions. Sensors and Actuators B: Chemical, 2013, 185, 488-495.	4.0	40

#	Article	IF	CITATIONS
73	Enhancement in hyperthermia efficiency under <i>in situ</i> orientation of superparamagnetic iron oxide nanoparticles in dispersions. Applied Physics Letters, 2019, 115, .	1.5	40
74	Effect of polymer-surfactant association on colloidal force. Physical Review E, 2002, 66, 011406.	0.8	39
75	Competitive adsorption of polymer and surfactant at a liquid droplet interface and its effect on flocculation of emulsion. Journal of Colloid and Interface Science, 2012, 366, 88-95.	5.0	39
76	Magnetorheological properties of a magnetic nanofluid with dispersed carbon nanotubes. Physical Review E, 2014, 89, 022310.	0.8	39
77	Synthesis of Stable Magnetic Nanofluids of Different Particle Sizes. Journal of Nanofluids, 2012, 1, 85-92.	1.4	39
78	Colloidal force measurements in the presence of a polyelectrolyte. Journal Physics D: Applied Physics, 1997, 30, 2798-2803.	1.3	38
79	Size-controlled synthesis of superparamagnetic magnetite nanoclusters for heat generation in an alternating magnetic field. Journal of Molecular Liquids, 2019, 281, 315-323.	2.3	38
80	The interaction, stability and response to an external stimulus of iron oxide nanoparticle–casein nanocomplexes. Colloids and Surfaces A: Physicochemical and Engineering Aspects, 2012, 406, 52-60.	2.3	37
81	Infrared thermography based defect detection in ferromagnetic specimens using a low frequency alternating magnetic field. Infrared Physics and Technology, 2014, 64, 125-133.	1.3	37
82	Uncertainties in the estimation of specific absorption rate during radiofrequency alternating magnetic field induced non-adiabatic heating of ferrofluids. Journal Physics D: Applied Physics, 2017, 50, 455005.	1.3	37
83	Facile fabrication of robust superhydrophobic aluminum surfaces with enhanced corrosion protection and antifouling properties. Progress in Organic Coatings, 2022, 162, 106560.	1.9	36
84	High temperature phase transformation studies in magnetite nanoparticles doped with Co2+ ion. Journal of Applied Physics, 2012, 112, .	1.1	34
85	Temperature and pH sensor based on functionalized magnetic nanofluid. Sensors and Actuators B: Chemical, 2018, 268, 338-349.	4.0	34
86	Pitting and stress corrosion cracking studies on AISI type 316N stainless steel weldments. Defence Technology, 2018, 14, 226-237.	2.1	34
87	Role of Adsorbing Moieties on Thermal Conductivity and Associated Properties of Nanofluids. Journal of Physical Chemistry C, 2013, 117, 9009-9019.	1.5	33
88	Experimental evidence for the significant role of initial cluster size and liquid confinement on thermo-physical properties of magnetic nanofluids under applied magnetic field. Journal of Molecular Liquids, 2018, 257, 1-11.	2.3	33
89	Magnetic nanofluid based non-enzymatic sensor for urea detection. Sensors and Actuators B: Chemical, 2018, 255, 720-728.	4.0	33
90	Effect of initial particle size on phase transformation temperature of surfactant capped Fe3O4 nanoparticles. Journal of Applied Physics, 2011, 109, .	1.1	32

#	Article	IF	CITATIONS
91	Effect of Nanoparticle Size, Morphology and Concentration on Specific Heat Capacity and Thermal Conductivity of Nanofluids. Journal of Nanofluids, 2015, 4, 302-309.	1.4	32
92	Optimal condition for fabricating mechanically durable superhydrophobic titanium surface by rapid breakdown anodization: Self cleaning and bouncing characteristics. Applied Surface Science, 2022, 585, 152628.	3.1	32
93	High temperature stability of surfactant capped CoFe2O4 nanoparticles. Materials Chemistry and Physics, 2011, 130, 1300-1306.	2.0	31
94	Functionalization of Iron Oxide Nanoparticles with Biosurfactants and Biocompatibility Studies. Journal of Biomedical Nanotechnology, 2013, 9, 751-764.	0.5	30
95	One-step microwave-assisted synthesis of water-dispersible Fe 3 O 4 magnetic nanoclusters for hyperthermia applications. Journal of Magnetism and Magnetic Materials, 2017, 439, 107-113.	1.0	30
96	Role of field-induced nanostructures, zippering and size polydispersity on effective thermal transport in magnetic fluids without significant viscosity enhancement. Journal of Magnetism and Magnetic Materials, 2017, 444, 29-42.	1.0	30
97	Corrosion inhibition of mild steel in 1 M HCl usingTamarindus indicaextract: electrochemical, surface and spectroscopic studies. Journal of Adhesion Science and Technology, 2020, 34, 713-743.	1.4	30
98	A Simple, In-Expensive and Ultrasensitive Magnetic Nanofluid Based Sensor for Detection of Cations, Ethanol and Ammonia. Journal of Nanofluids, 2013, 2, 112-119.	1.4	29
99	Naked eye visualization of defects in ferromagnetic materials and components. NDT and E International, 2013, 60, 100-109.	1.7	28
100	An optical technique for fast and ultrasensitive detection of ammonia using magnetic nanofluids. Applied Physics Letters, 2013, 102, .	1.5	28
101	A facile approach to enhance the high temperature stability of magnetite nanoparticles with improved magnetic property. Journal of Applied Physics, 2013, 113, .	1.1	28
102	Infrared thermography based magnetic hyperthermia study in Fe3O4 based magnetic fluids. Infrared Physics and Technology, 2016, 78, 173-184.	1.3	28
103	Optical investigations in the various phases of an antiferroelectric liquid crystal. Physical Review E, 1995, 52, 1846-1856.	0.8	27
104	Comparison of light scattering from self assembled array of nanoparticle chains with cylinders. Optics Communications, 2012, 285, 1242-1247.	1.0	27
105	Preparation, characterization and X-ray attenuation property of Gd2O3-based nanocomposites. Applied Nanoscience (Switzerland), 2017, 7, 919-931.	1.6	27
106	Effect of orientational ordering of magnetic nanoemulsions immobilized in agar gel on magnetic hyperthermia. Journal of Magnetism and Magnetic Materials, 2018, 451, 254-268.	1.0	27
107	The chloride-induced corrosion of a fly ash concrete with nanoparticles and corrosion inhibitor. Construction and Building Materials, 2021, 274, 122097.	3.2	27
108	Efficient Dye Degradation via Catalytic Persulfate Activation using Iron Oxide-Manganese Oxide Core-Shell Particle Doped with Transition Metal Ions. Journal of Molecular Liquids, 2021, 337, 116429.	2.3	27

#	Article	IF	CITATIONS
109	High magnetic fluid hyperthermia efficiency in copper ferrite nanoparticles prepared by solvothermal and hydrothermal methods. Journal of Magnetism and Magnetic Materials, 2021, 538, 168233.	1.0	27
110	Fabrication of a robust graphene oxide-nano SiO2-polydimethylsiloxane composite coating on carbon steel for marine applications. Progress in Organic Coatings, 2021, 161, 106462.	1.9	27
111	Probing of Field-Induced Structures and Their Dynamics in Ferrofluids Using Oscillatory Rheology. Langmuir, 2014, 30, 12171-12179.	1.6	26
112	Study of the tensile behavior of AISI type 316 stainless steel using acoustic emission and infrared thermography techniques. Journal of Materials Research and Technology, 2015, 4, 241-253.	2.6	26
113	Structural stability of ZnFe2O4 nanoparticles under different annealing conditions. Materials Chemistry and Physics, 2011, 128, 400-404.	2.0	25
114	Enhanced thermal stability of phosphate capped magnetite nanoparticles. Journal of Applied Physics, 2014, 115, 224304.	1.1	25
115	Thermal conductivity measurements in phase change materials under freezing in presence of nanoinclusions. Journal of Applied Physics, 2015, 118, .	1.1	25
116	Fabrication of silanized GO hybrid coating on 316L SS with enhanced corrosion resistance and antibacterial properties for marine applications. Surface and Coatings Technology, 2020, 402, 126295.	2.2	25
117	Condition monitoring of exhaust system blowers using infrared thermography. Insight: Non-Destructive Testing and Condition Monitoring, 2008, 50, 512-515.	0.3	24
118	Anomalous enhancement of corrosion resistance and antibacterial property of commercially pure Titanium (CP-Ti) with nanoscale rutile titania film. Corrosion Science, 2020, 172, 108678.	3.0	24
119	Thermal and rheological properties of magnetic nanofluids: Recent advances and future directions. Advances in Colloid and Interface Science, 2022, 307, 102729.	7.0	24
120	Non-destructive Evaluation of Friction Stir Welded Joints by X-ray Radiography and Infrared Thermography. Procedia Engineering, 2014, 86, 469-475.	1.2	23
121	A Simple Approach to Produce Stable Ferrofluids Without Surfactants and With High Temperature Stability. Journal of Nanofluids, 2013, 2, 94-103.	1.4	23
122	Viscous Sintering Phenomena in Liquid-Liquid Dispersions. Physical Review Letters, 2000, 84, 2018-2021.	2.9	22
123	Tunable Thermal Transport in Phase Change Materials Using Inverse Micellar Templating and Nanofillers. Journal of Physical Chemistry C, 2014, 118, 13972-13980.	1.5	22
124	Thermally tunable grating using thermo-responsive magnetic fluid. Optical Materials, 2017, 66, 117-121.	1.7	22
125	Enhanced corrosion protection of reinforcement steel with nanomaterial incorporated fly ash based cementitious coating. Construction and Building Materials, 2021, 275, 122130.	3.2	22
126	Synthesis, Characterization, Thermal Conductivity and Rheological Studies in Magnetite-Decorated Graphene Oxide Nanofluids. Journal of Nanofluids, 2018, 7, 11-20.	1.4	22

#	Article	IF	CITATIONS
127	Biosynthesis and Functionalization of Silver Nanoparticles Using <i>Nigellasativa</i> , <i>Dioscorea alata</i> and <i>Ferula asafoetida</i> . Science of Advanced Materials, 2014, 6, 1681-1690.	0.1	22
128	Size distribution of magnetic iron oxide nanoparticles using Warren–Averbach XRD analysis. Journal of Physics and Chemistry of Solids, 2012, 73, 867-872.	1.9	21
129	Non-enzymatic glucose detection using magnetic nanoemulsions. Applied Physics Letters, 2014, 105, 123110.	1.5	21
130	Microwave Assisted Synthesis of Ferrite Nanoparticles: Effect of Reaction Temperature on Particle Size and Magnetic Properties. Journal of Nanoscience and Nanotechnology, 2015, 15, 5768-5774.	0.9	21
131	A new ternary composite steel rebar coating for enhanced corrosion resistance in chloride environment. Construction and Building Materials, 2022, 320, 126307.	3.2	21
132	Electro-optic Kerr effect studies in liquids and binary liquid mixtures Journal of Molecular Liquids, 1991, 48, 85-97.	2.3	20
133	Effect of Surface Functionalization and Physical Properties of Nanoinclusions on Thermal Conductivity Enhancement in an Organic Phase Change Material. ACS Omega, 2018, 3, 9487-9504.	1.6	20
134	Enhanced magnetic heating efficiency at acidic pH for magnetic nanoemulsions stabilized with a weak polyelectrolyte. Journal of Colloid and Interface Science, 2020, 579, 582-597.	5.0	20
135	Rupturing of bitumen-in-water emulsions: experimental evidence for viscous sintering phenomena. Colloids and Surfaces A: Physicochemical and Engineering Aspects, 2001, 176, 185-194.	2.3	19
136	Biocompatibility Studies of Functionalized CoFe2O4 Magnetic Nanoparticles. Current Nanoscience, 2011, 7, 371-376.	0.7	19
137	Multi-stimuli responsive nanofluid with easy-to-visualize structural color patterns. Colloids and Surfaces A: Physicochemical and Engineering Aspects, 2017, 518, 98-108.	2.3	19
138	Magnetorheological properties of sodium sulphonate capped electrolytic iron based MR fluid: a comparison with CI based MR fluid. Smart Materials and Structures, 2017, 26, 025003.	1.8	19
139	Temporal evolution of equilibrium and non-equilibrium magnetic field driven microstructures in a magnetic fluid. Journal of Molecular Liquids, 2020, 304, 112737.	2.3	19
140	Fabrication of superhydrophobic and self cleaning <scp>PVAâ€silica</scp> fiber coating on <scp>304L SS</scp> surfaces by electrospinning. Journal of Applied Polymer Science, 2021, 138, 50118.	1.3	19
141	Long term antifouling performance of superhydrophobic surfaces in seawater environment: Effect of substrate material, hierarchical surface feature and surface chemistry. Colloids and Surfaces A: Physicochemical and Engineering Aspects, 2022, 647, 129194.	2.3	19
142	Transient Kerr response in a nematic liquid crystal. Journal Physics D: Applied Physics, 1992, 25, 1231-1234.	1.3	18
143	Thermogelling Properties of Triblock Copolymers in the Presence of Hydrophilic Fe <sub>3</sub> O <sub>4</sub> Nanoparticles and Surfactants. Langmuir, 2012, 28, 12044-12053.	1.6	18
144	Detection of pathogenic gram negative bacteria using infrared thermography. Infrared Physics and Technology, 2012, 55, 485-490.	1.3	18

#	Article	IF	CITATIONS
145	Near infrared light absorption in magnetic nanoemulsion under external magnetic field. Optics Communications, 2014, 323, 54-60.	1.0	18
146	Infrared thermography based studies on mobile phone induced heating. Infrared Physics and Technology, 2015, 71, 242-251.	1.3	18
147	Impact of field ramp rate on magnetic field assisted thermal transport in ferrofluids. Journal of Molecular Liquids, 2020, 298, 112047.	2.3	18
148	Kerr effect studies in acetonitrile-aromatic hydrocarbon systems. Journal of Molecular Liquids, 1991, 50, 115-124.	2.3	17
149	Development of active magnetic bearings and ferrofluid seals toward oil free sodium pumps. Nuclear Engineering and Design, 2013, 265, 1166-1174.	0.8	17
150	Magnetic field dependant backscattering of light in water based ferrofluid containing polymer covered Fe3O4 nanoparticles. Journal of Applied Physics, 2013, 113, .	1.1	17
151	External magnetic field dependent light transmission and scattered speckle pattern in a magnetically polarizable oil-in-water nanoemulsion. Physica B: Condensed Matter, 2014, 454, 272-278.	1.3	17
152	Polydimethylsiloxane–graphene oxide nanocomposite coatings with improved anti-corrosion and anti-biofouling properties. Environmental Science and Pollution Research, 2021, 28, 7404-7422.	2.7	17
153	Segmentation of defects from radiography images by the histogram concavity threshold method. Insight: Non-Destructive Testing and Condition Monitoring, 2007, 49, 578-584.	0.3	16
154	Dependence of particle size on the effective thermal diffusivity and conductivity of nanofluids: role of base fluid properties. Heat and Mass Transfer, 2012, 48, 1783-1790.	1.2	16
155	Preparation of metal oxide nanoparticles of different sizes and morphologies, their characterization using small angle X-ray scattering and study of thermal properties. Materials Chemistry and Physics, 2014, 145, 213-221.	2.0	16
156	Nano-inclusion aided thermal conductivity enhancement in palmitic acid/di-methyl formamide phase change material for latent heat thermal energy storage. Thermochimica Acta, 2019, 678, 178309.	1.2	16
157	Efficacy of imidazolium and piperidinium based ionic liquids on inhibiting biofilm formation on titanium and carbon steel surfaces. Analytica Chimica Acta, 2020, 1126, 38-51.	2.6	16
158	Polymer nanocomposites containing βâ€Bi <sub>2</sub> O <sub>3</sub> and silica nanoparticles: Thermal stability, surface topography and Xâ€ray attenuation properties. Journal of Applied Polymer Science, 2020, 137, 49048.	1.3	16
159	Infrared thermography based studies on the effect of age on localized cold stress induced thermoregulation in human. Infrared Physics and Technology, 2016, 76, 592-602.	1.3	15
160	Thermal Stability and X-ray Attenuation Studies on <i>α</i> Bi <sub>2</sub> O <sub>3</sub> , <i>β</i> Bi <sub>2</sub> O <sub>3</sub> and Bi Based Nanocomposites for Radiopaque Fabrics. Journal of Nanoscience and Nanotechnology, 2018, 18, 3969-3981.	0.9	15
161	Enhancement in field induced heating efficiency of TMAOH coated superparamagnetic Fe3O4 nanoparticles by texturing under a static bias field. Journal of Magnetism and Magnetic Materials, 2020, 498, 166138.	1.0	15
162	Gelation and Coarsening in Dispersions of Highly Viscous Droplets. Langmuir, 2001, 17, 3545-3552.	1.6	14

#	Article	IF	CITATIONS
163	Spectral response of magnetic nanofluid to toxic cations. Applied Physics Letters, 2013, 102, .	1.5	14
164	Influence of Ag <sup>+</sup> Interaction on 1D Droplet Array Spacing and the Repulsive Forces between Stimuli-Responsive Nanoemulsion Droplets. Langmuir, 2014, 30, 10213-10220.	1.6	14
165	Irradiation performance of PFBR MOX fuel after 112GWd/t burn-up. Journal of Nuclear Materials, 2014, 449, 31-38.	1.3	14
166	Online monitoring of cutting tool temperature during micro-end milling using infrared thermography. Insight: Non-Destructive Testing and Condition Monitoring, 2015, 57, 9-17.	0.3	14
167	Superior thermal stability of polymer capped Fe <sub>3</sub> O <sub>4</sub> magnetic nanoclusters. Journal of the American Ceramic Society, 2018, 101, 483-491.	1.9	14
168	Behavior of a Weak Polyelectrolyte at Oil-water Interfaces under Different Environmental Conditions. Colloids and Surfaces A: Physicochemical and Engineering Aspects, 2018, 538, 610-621.	2.3	14
169	Field induced deformation of sessile ferrofluid droplets: Effect of particle size distribution on magnetowetting. Journal of Magnetism and Magnetic Materials, 2018, 466, 295-300.	1.0	14
170	Antibacterial and Corrosion Studies on Nanosecond Pulse Laser Textured 304ÂL Stainless Steel Surfaces. Lasers in Manufacturing and Materials Processing, 2019, 6, 332-343.	1.2	14
171	Determination of nanoscale titanium oxide thin film phase composition using X-ray photoelectron spectroscopy valence band analysis. Thin Solid Films, 2019, 681, 58-68.	0.8	14
172	Atmospheric air oxidation of 9Cr-1Mo steel: Depth profiling of oxide layers using glow discharge optical emission spectrometry. Spectrochimica Acta, Part B: Atomic Spectroscopy, 2020, 172, 105973.	1.5	14
173	Synthesis of water dispersible phosphate capped CoFe2O4 nanoparticles and its applications in efficient organic dye removal. Colloids and Surfaces A: Physicochemical and Engineering Aspects, 2021, 610, 125755.	2.3	14
174	Graphene oxide/polyvinylpyrrolidone composite coating on 316L SS with superior antibacterial and anti-biofouling properties. Progress in Organic Coatings, 2021, 158, 106356.	1.9	14
175	A simple approach for fabrication of superhydrophobic titanium surface with self-cleaning and bouncing properties. Colloids and Surfaces A: Physicochemical and Engineering Aspects, 2022, 636, 128110.	2.3	14
176	Enhanced transmission with tunable Fano-like profile in magnetic nanofluids. Physical Review E, 2011, 84, 051403.	0.8	13
177	Measurement of annular air-gap using active infrared thermography. Infrared Physics and Technology, 2013, 61, 192-199.	1.3	13
178	Behavior of a strong polyelectrolyte, poly(diallyldimethylammonium chloride) physisorbed at oil-water interface under different environments : A comparison with a weak polyelectrolyte. Colloids and Surfaces A: Physicochemical and Engineering Aspects, 2018, 550, 209-221.	2.3	13
179	Phase identification in binary mixture of nanopowders from deconvoluted valence band spectra using X-ray photoelectron spectroscopy: Case study with iron oxide and titania polymorphs. Applied Surface Science, 2018, 462, 932-943.	3.1	13
180	Electrophoretically deposited graphene oxide–polymer bilayer coating on Cu-Ni alloy with enhanced corrosion resistance in simulated chloride environment. Journal of Coatings Technology Research, 2019, 16, 1317-1335.	1.2	13

#	Article	IF	CITATIONS
181	Effect of initial susceptibility and relaxation dynamics on radio frequency alternating magnetic field induced heating in superparamagnetic nanoparticle dispersions. Journal of Magnetism and Magnetic Materials, 2019, 486, 165267.	1.0	13
182	Oil-absorbent MnOx capped iron oxide nanoparticles: Synthesis, characterization and applications in oil recovery. Journal of Molecular Liquids, 2020, 320, 114324.	2.3	13
183	Influence of size polydispersity on magnetic field tunable structures in magnetic nanofluids containing superparamagnetic nanoparticles. Nanoscale Advances, 2021, 3, 3573-3592.	2.2	13
184	Development of X-ray protective garments from rare earth-modified natural rubber composites. Journal of Elastomers and Plastics, 2017, 49, 527-544.	0.7	12
185	Microstructure, corrosion and mechanical properties characterization of AISI type 316L(N) stainless steel and modified 9Cr-1Mo steel after 40,000†h of dynamic sodium exposure at 525†°C. Journal of Nuclear Materials, 2019, 516, 84-99.	1.3	12
186	Enhanced biodeterioration and biofouling resistance of nanoparticles and inhibitor admixed fly ash based concrete in marine environments. International Biodeterioration and Biodegradation, 2020, 155, 105088.	1.9	12
187	Enhanced Thermal Protection of Iron Oxide Nanoparticle by Insulating Nanoporous Char Layer: Effect of Core Size and Char Layer Properties. Journal of Physical Chemistry C, 2020, 124, 5702-5714.	1.5	12
188	Effect of Surfactant on the Size, Zeta Potential and Rheology of Alumina Nanofluids. Journal of Nanofluids, 2014, 3, 328-335.	1.4	12
189	A high-voltage pulse measuring system based on the Kerr effect. Measurement Science and Technology, 1991, 2, 565-567.	1.4	11
190	Transient kerr effect in nematic liquid crystal mixtures. Journal of Molecular Liquids, 1991, 50, 215-223.	2.3	11
191	A Single Pot Approach for Synthesis of Phosphate Coated Iron Oxide Nanoparticles. Journal of Nanoscience and Nanotechnology, 2015, 15, 2715-2725.	0.9	11
192	Temperature dependent light transmission in ferrofluids. Optics Communications, 2015, 342, 224-229.	1.0	11
193	Probing of Competitive Displacement Adsorption of Casein at Oil-in-Water Interface Using Equilibrium Force Distance Measurements. Journal of Physical Chemistry B, 2015, 119, 6828-6835.	1.2	11
194	A spectroscopic approach to probe macromolecular conformational changes at interface under different environmental conditions: A case study with PAA adsorbed at oil-water Interface. Journal of Molecular Liquids, 2018, 252, 30-39.	2.3	11
195	Stability and rheological properties of hybrid Î <sup>3</sup> -Al2O3 nanofluids with cationic polyelectrolyte additives. Colloids and Surfaces A: Physicochemical and Engineering Aspects, 2018, 555, 63-71.	2.3	11
196	Adsorption of bovine serum albumin at oil-water interface in the presence of polyelectrolytes and nature of interaction forces. Colloids and Surfaces A: Physicochemical and Engineering Aspects, 2019, 566, 38-47.	2.3	11
197	SENSORS FOR MONITORING COMPONENTS, SYSTEMS AND PROCESSES. International Journal on Smart Sensing and Intelligent Systems, 2010, 3, 61-74.	0.4	11
198	Irradiation Behavior of FBTR Mixed Carbide Fuel at Various Burn-ups. Energy Procedia, 2011, 7, 227-233.	1.8	10

#	Article	IF	CITATIONS
199	In situ application of alternate potentials with chlorination synergistically enhanced biofouling control of titanium condenser materials. International Biodeterioration and Biodegradation, 2019, 144, 104746.	1.9	10
200	Effect of surface charge screening on critical magnetic fields during field induced structural transitions in magnetic fluids. Journal of Applied Physics, 2019, 125, .	1.1	10
201	Synergistic effect of β-Bi2O3 and graphene/MWCNT in silicone-based polymeric matrices on diagnostic X-ray attenuation. Applied Nanoscience (Switzerland), 2019, 9, 1891-1913.	1.6	10
202	A facile approach to synthesis of cobalt ferrite nanoparticles with a uniform ultrathin layer of silicon carbide for organic dye removal. Journal of Molecular Liquids, 2020, 317, 114110.	2.3	10
203	Visual detection of defects in carbon steel using magnetic nanoemulsions: Effect of stabilizing moieties on the defect detection sensitivity. Sensors and Actuators A: Physical, 2020, 314, 112220.	2.0	10
204	In Situ Raman Spectroscopic Analysis on Carbon Steel, Immersed in Aqueous Solutions at Different pH and Anions. Journal of Materials Engineering and Performance, 2020, 29, 2792-2805.	1.2	10
205	Magnetic hyperthermia studies in magnetite ferrofluids based on bio-friendly oils extracted from Calophyllum inophyllum, Brassica juncea, Ricinus communis and Madhuca longifolia. Journal of Magnetism and Magnetic Materials, 2021, 537, 168134.	1.0	10
206	High-Temperature Air and Steam Oxidation and Oxide Layer Characteristics of Alloy 617. Journal of Materials Engineering and Performance, 2021, 30, 931-943.	1.2	10
207	Rheological Properties of Magnetorheological Fluid with Silica Nanoparticles Stabilizers—A Comparison with Ferrofluid. Journal of Nanofluids, 2013, 2, 75-84.	1.4	10
208	Synthesis of Silver Capped Fe <sub>3</sub> O <sub>4</sub> Nanofluids Using Microwave Assisted Approach. Journal of Nanofluids, 2017, 6, 1-10.	1.4	10
209	Microwave Assisted Synthesis of Magnetite Nanoparticles. Journal of Nanoscience and Nanotechnology, 2014, 14, 5790-5797.	0.9	9
210	Effect of non-magnetic inclusions in magnetic specimens on defect detection sensitivity using active infrared thermography. Infrared Physics and Technology, 2015, 68, 52-60.	1.3	9
211	Infrared Thermography for Detection of Diabetic Neuropathy and Vascular Disorder. Series in Bioengineering, 2017, , 217-247.	0.3	9
212	Multifiller nanocomposites containing gadolinium oxide and bismuth nanoparticles with enhanced Xâ€ray attenuation property. Journal of Applied Polymer Science, 2021, 138, 51252.	1.3	9
213	Role of Oxygen Vacancy Formation Energy and Insulating Behavior in Darkening of White Amorphous TiO <sub>2</sub> . Journal of Physical Chemistry C, 2021, 125, 16136-16146.	1.5	9
214	Inter-droplet force between magnetically polarizable Pickering oil-in-water nanoemulsions stabilized with γ-Al2O3 nanoparticles: Role of electrostatic and electric dipolar interactions. Journal of Colloid and Interface Science, 2022, 607, 1671-1686.	5.0	9
215	Synthesis and magneto-structural properties of chitosan coated ultrafine cobalt ferrite nanoparticles for magnetic fluid hyperthermia in viscous medium. Ceramics International, 2022, 48, 22767-22781.	2.3	9
216	Forces between colloidal droplets in the presence of a weak polyelectrolyte. Bulletin of Materials Science, 1999, 22, 313-320.	0.8	8

#	Article	IF	CITATIONS
217	Effect of Precipitating Agent and Solvent Polarity on the Size and Magnetic Properties of Magnetite Nanoparticles Prepared by Microwave Assisted Synthesis. Journal of Nanoscience and Nanotechnology, 2016, 16, 9591-9602.	0.9	8
218	Investigations on magnetic field induced optical transparency in magnetic nanofluids. Optical Materials, 2018, 76, 97-105.	1.7	8
219	Fungal resistance of nanomodifiers and corrosion inhibitor amended fly ash concrete. International Biodeterioration and Biodegradation, 2019, 143, 104725.	1.9	8
220	Porous Microcapsule-Based Regenerating Superhydrophobic Coating on 304L SS and Its Corrosion Properties. Journal of Materials Engineering and Performance, 2019, 28, 7047-7057.	1.2	8
221	Microstructural and phase characterisation of pyrolytic graphite coating by CVD using propane and methane as precursor. Materials at High Temperatures, 2019, 36, 540-547.	0.5	8
222	Corrosion Evaluation of Buried Cast Iron Pipes Exposed to Fire Water System for 30Âyears. Transactions of the Indian Institute of Metals, 2020, 73, 9-21.	0.7	8
223	Observation of soft glassy behavior in a magnetic colloid exposed to an external magnetic field. Soft Matter, 2020, 16, 7126-7136.	1.2	8
224	Binary blended fly ash concrete with improved chemical resistance in natural and industrial environments. Environmental Science and Pollution Research, 2021, 28, 28107-28132.	2.7	8
225	Effect of Polymeric Additives on Thermal and Electrical Conductivity of Nanofluids. Journal of Nanofluids, 2016, 5, 661-668.	1.4	8
226	An optical technique for the detection of surface defects in ferromagnetic samples. Measurement Science and Technology, 1999, 10, N71-N75.	1.4	7
227	Thermal conduction in polymeric nanofluids under mean field approximation: role of interfacial adsorption layers. Physica Scripta, 2013, 88, 015602.	1.2	7
228	Comparison of magnetic properties and high-temperature phase stability of phosphate- and oleic acid-capped iron oxide nanoparticles. Applied Nanoscience (Switzerland), 2018, 8, 593-608.	1.6	7
229	Development of Superhydrophobic Coating on Copper for Enhanced Corrosion Resistance in Chloride Medium. Transactions of the Indian Institute of Metals, 2019, 72, 1133-1143.	0.7	7
230	Enhanced antiâ€microbial activity in green concrete specimens containing fly ash, nanophase modifiers, and corrosion inhibitor. Environmental Progress and Sustainable Energy, 2019, 38, 13102.	1.3	7
231	Effect of Nitrogen on the Intergranular Stress Corrosion Cracking Resistance of 316LN Stainless Steel. Corrosion, 2020, 76, 591-600.	0.5	7
232	Comparison between the tilted SmC?* and SmC?* phases of MHPOBC studied by optical techniques. Journal De Physique II, 1994, 4, 2149-2159.	0.9	7
233	Tuning magnetic heating efficiency of colloidal dispersions of iron oxide nano-clusters by varying the surfactant concentration during solvothermal synthesis. Journal of Molecular Liquids, 2022, 360, 119444.	2.3	7
234	Thermal diffusion in dilute nanofluids investigated by photothermal interferometry. Journal of Physics: Conference Series, 2010, 214, 012035.	0.3	6

#	Article	IF	CITATIONS
235	Evaluation of dissimilar friction stir lap joints using digital X-ray radiography. Science and Technology of Welding and Joining, 2014, 19, 125-132.	1.5	6
236	Infrared thermal imaging based study of localized cold stress induced thermoregulation in lower limbs: The role of age on the inversion time. Journal of Thermal Biology, 2020, 94, 102781.	1.1	6
237	Poly acrylic acid stabilized magnetic nanoemulsions for visual defect detection: Effect of pH on detection sensitivity and colloidal stability. Journal of Molecular Liquids, 2021, 336, 116332.	2.3	6
238	Nature of Alkali Used in the Co-Precipitation of Superparamagnetic Nanoparticles on Their Thermal Stability and the Properties of Ferrofluids. Journal of Nanofluids, 2012, 1, 128-136.	1.4	6
239	Transmitted Light Intensity and the Speckle Pattern in a Poly-Acrylic Acid Stabilized Ferrofluid in the Presence of an External Magnetic Field. Journal of Nanofluids, 2013, 2, 237-248.	1.4	6
240	Kerr effect in binary liquid mixtures. Journal of Molecular Liquids, 1991, 50, 207-214.	2.3	5
241	Nonresonant third order susceptibility measurements in a nematic liquid crystalâ€PCHâ€5. Journal of Applied Physics, 1992, 72, 1495-1497.	1.1	5
242	Electrooptical Kerr constant and third-order susceptibility measurements in nematic liquid crystals and their mixtures. Optical and Quantum Electronics, 1992, 24, 825-832.	1.5	5
243	Nonresonant third-order susceptibility measurements in the nematic liquid crystal K18. Optical and Quantum Electronics, 1993, 25, 157-162.	1.5	5
244	Anisotropic Rayleigh scattering investigations in smecticAliquid crystal phases. Journal of Chemical Physics, 1994, 101, 6301-6317.	1.2	5
245	Highly crystalline core-shell FeCo-CoFe <sub>2</sub> O <sub>4</sub> nanostructures. EPJ Applied Physics, 2013, 63, 30401.	0.3	5
246	Effect of Cation Trapping on Thermal Stability of Magnetite Nanoparticles. Journal of Nanoscience and Nanotechnology, 2014, 14, 4114-4123.	0.9	5
247	Infrared thermography-based studies on hydrotesting of stainless steel pressure vessels. Insight: Non-Destructive Testing and Condition Monitoring, 2015, 57, 406-413.	0.3	5
248	Studies on the Susceptibility of Modified 9Cr-1Mo Steel to Stress Corrosion Cracking in Sodium Hydroxide Using Slow Strain Rate Testing Technique. Journal of Materials Engineering and Performance, 2020, 29, 2172-2184.	1.2	5
249	Synthesis of Ni doped iron oxide colloidal nanocrystal clusters using poly(N-isopropylacrylamide) templates for efficient recovery of cefixime and methylene blue. Colloids and Surfaces A: Physicochemical and Engineering Aspects, 2022, 650, 129616.	2.3	5
250	Image processing of radiographs of tube-to-tubesheet weld joints for enhanced detectability of defects. Insight: Non-Destructive Testing and Condition Monitoring, 2008, 50, 298-303.	0.3	4
251	Enhanced sensitivity detection of defects in gas turbine blades of aero-engine and hairpin tubes of heavy water plant using microfocal radiography. Insight: Non-Destructive Testing and Condition Monitoring, 2008, 50, 560-563.	0.3	4
252	Temperature-Induced Gelation in Dilute Nanofluids. Langmuir, 2011, 27, 12361-12367.	1.6	4

#	Article	IF	CITATIONS
253	Dimensional measurements on 112GWd/t irradiated MOX fuel pins using X-ray radiography. Annals of Nuclear Energy, 2015, 83, 8-13.	0.9	4
254	Macromolecular conformation changes at oil-water interface in the presence of cations. Colloids and Surfaces A: Physicochemical and Engineering Aspects, 2016, 497, 90-100.	2.3	4
255	Rapid removal of rhodamine dye from aqueous solution using casein-surfactant complexes: role of casein-surfactant interaction. Journal of Dispersion Science and Technology, 2020, , 1-16.	1.3	4
256	Enhancing the Intergranular Corrosion Resistance of High-Nitrogen-Containing 316L Stainless Steels by Grain Boundary Engineering via Thermomechanical Treatment. Corrosion, 2020, 76, 835-842.	0.5	4
257	Reconfiguring nanostructures in magnetic fluids using pH and magnetic stimulus for tuning optical properties. Journal of Magnetism and Magnetic Materials, 2021, 539, 168351.	1.0	4
258	Studies on localized electrochemical activity of 304L SS-Zr-4 dissimilar joints using alternating current scanning electrochemical microscopy. Applied Surface Science, 2022, 578, 151958.	3.1	4
259	Magnetic nanoemulsion aided optical defect detection in carbon steel components: Effect of defect width variation on optical contrast. Journal of Applied Physics, 2022, 131, .	1.1	4
260	Laser based etching technique for metallography and ceramography. Materials Science & Engineering A: Structural Materials: Properties, Microstructure and Processing, 2002, 338, 17-23.	2.6	3
261	Enhancement in maghemite to hematite phase transition temperature with very low fraction of Co (II) doping. , 2011, , .		3
262	Role of surface charge, morphology, and adsorbed moieties on thermal conductivity enhancement of nanofluids. Applied Physics Letters, 2012, 101, 173113.	1.5	3
263	Path length tunable light-matter interaction in magnetic nanofluid based field-induced photonic crystal-glass structure. New Journal of Physics, 2016, 18, 103037.	1.2	3
264	Functionalization of Cobalt Ferrite Nanoparticles with Biotin and Lawsone and Their Use in Rhodamine Dye and Lead Ion Removal. Journal of Nanoscience and Nanotechnology, 2017, 17, 5284-5293.	0.9	3
265	Magnetic hyperthermia in water based ferrofluids: Effects of initial susceptibility and size polydispersity on heating efficiency. AIP Conference Proceedings, 2018, , .	0.3	3
266	Pitting Corrosion Studies on Fusion Zone of Shielded Metal Arc Welded Type 316LN Stainless Steel Weldments. Transactions of the Indian Institute of Metals, 2019, 72, 3089-3105.	0.7	3
267	Studies Using Force, Hydrodynamic Size and Zeta Potential Measurements on Complexation of Polymer and Surfactant on Emulsion Interface. Journal of Colloid Science and Biotechnology, 2012, 1, 51-59.	0.2	3
268	Microwave Assisted Synthesis of Ferrite Nanoparticles and Nanofluids with Tunable Curie Temperature. Journal of Nanofluids, 2014, 3, 210-216.	1.4	3
269	Influence of long term Sodium Exposure on the Corrosion and Tensile Properties of AISI Type 316LN stainless steel and modified 9Cr-1Mo steel. Journal of Nuclear Materials, 2022, 567, 153830.	1.3	3
270	Effective thermal conductivity of condensed polymeric nanofluids (nanosolids) controlled by diffusion and interfacial scattering. Pramana - Journal of Physics, 2013, 81, 849-864.	0.9	2

#	Article	IF	CITATIONS
271	Simulation of beam hardening in X-ray tomography and its correction using linearisation and pre-filtering approaches. Insight: Non-Destructive Testing and Condition Monitoring, 2013, 55, 540-547.	0.3	2
272	Studies on temperature evolution during fatigue cycling of Ni-Al bronze (NAB) alloy using infrared thermography. Insight: Non-Destructive Testing and Condition Monitoring, 2016, 58, 70-81.	0.3	2
273	Development of a Sulfamic Acid-Based Chemical Formulation for Effective Cleaning of Modified 9Cr–1Mo Steel Steam Generator Tubes. Transactions of the Indian Institute of Metals, 2020, 73, 343-352.	0.7	2
274	Failure of Printed Circuit Boards during Storage and Service: Leaked Capacitors and White Residue. Journal of Materials Engineering and Performance, 2020, 29, 6402-6411.	1.2	2
275	Effect of Molybdenum on Pit Initiation Rate and Pit Growth Using Electrochemical Noise and Its Correlation with Confocal Laser Scanning Microscopic Studies. Journal of Materials Engineering and Performance, 2020, 29, 5337-5345.	1.2	2
276	In-Situ Detection of Early Corrosion of Ferritic Cr-Mo Steel in Aqueous Solutions of different Anions using Laser Raman Spectroscopy. Journal of the Electrochemical Society, 2021, 168, 041508.	1.3	2
277	Magnetic Nanofluid Based Approach for Imaging Defects. Journal of Nanofluids, 2013, 2, 165-174.	1.4	2
278	Some aspects of pitting corrosion susceptibility of Asâ€welded and thermally aged nitrogenâ€alloyed 316SS weld metal. Materials and Corrosion - Werkstoffe Und Korrosion, 0, , .	0.8	2
279	Evaluation of Thermal Cycling Performance of Plasma Sprayed Alumina Coating on Inconel 600 with Different Bond Coats. Journal of Materials Engineering and Performance, 2022, 31, 4406-4418.	1.2	2
280	Nonresonant Third-Order Susceptibility Measurements in 4'-(Pentyloxy)-4-Biphenyl Carbonitrile (5OCB). Japanese Journal of Applied Physics, 1993, 32, 3493-3495.	0.8	1
281	Third-order Susceptibility Measurements in a Nematic Liquid Crystal—K15. Journal of Modern Optics, 1993, 40, 163-168.	0.6	1
282	Automatic detection and sizing of pores from radiographic images using the Hough transform. Insight: Non-Destructive Testing and Condition Monitoring, 2010, 52, 540-547.	0.3	1
283	Improved estimation of density of boron carbide control rods using digital X-ray radiography. Insight: Non-Destructive Testing and Condition Monitoring, 2011, 53, 258-262.	0.3	1
284	Effect of exposure and scattering on signal-to-noise ratio for improved defect sensitivity in X-ray radiography. Insight: Non-Destructive Testing and Condition Monitoring, 2013, 55, 548-552.	0.3	1
285	Influence of Casting Defects on S–N Fatigue Behavior of Ni-Al Bronze. Metallurgical and Materials Transactions A: Physical Metallurgy and Materials Science, 2015, 46, 708-725.	1.1	1
286	A Novel Approach to Enhance High Temperature Thermal Stability of Superparamagnetic Fe <sub>3</sub> O <sub>4</sub> Nanoparticles. Journal of Nanoscience and Nanotechnology, 2019, 19, 5624-5632.	0.9	1
287	Thermal Conductivity and Rheological Behaviour of Al-alloy Dispersed Ethylene Glycol Based Nanofluids. Journal of ASTM International, 2012, 9, 1-13.	0.2	1
288	Probing concentration and time dependent conformational changes in poly acrylic acid stabilized magnetic nanoemulsion using magnetic chaining-based inter-droplet force measurement. Colloids and Interface Science Communications, 2022, 47, 100592.	2.0	1

#	Article	IF	CITATIONS
289	X-ray radiography for development of defect-free electrochemical hydrogen meter for sodium systems. Insight: Non-Destructive Testing and Condition Monitoring, 2006, 48, 597-602.	0.3	0
290	Improved estimation of radial and axial gap of fuel pins from radiography images using image processing tools. Insight: Non-Destructive Testing and Condition Monitoring, 2007, 49, 701-707.	0.3	0
291	Non-destructive evaluation – a tool to identify genuine shaligram. Insight: Non-Destructive Testing and Condition Monitoring, 2010, 52, 13-15.	0.3	0
292	Optical sensing of salinity of water using magnetic nanoemulsions. , 2015, , .		0
293	On the durability of Pt coated Ti electrodes for the electro-oxidative dissolution of spent nuclear fuels. Corrosion Engineering Science and Technology, 2020, 55, 48-56.	0.7	0
294	Radio frequency magnetic field induced heating of superparamagnetic nanoparticle dispersions: Probing the interplay between anisotropy and dipolar energy. AIP Conference Proceedings, 2020, , .	0.3	0
295	Thermal Conductivity and Rheological Behaviour of Al-alloy Dispersed Ethylene Glycol Based Nanofluids. , 2012, , 104-121.		0
296	Microwave Assisted Biosynthesis of Magnetic Nanofluid Using Corn Extract. Journal of Nanofluids, 2013, 2, 307-315.	1.4	0